

The electrochemical regeneration of Fenton's reagent in the hydroxylation of aromatic substrates: batch and continuous processes

T. TZEDAKIS, A. SAVALL, M. J. CLIFTON

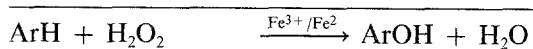
Laboratoire de Chimie-Physique et Electrochimie, (U.R.A. CNRS 192), Université Paul Sabatier, 31062 Toulouse cedex, France

Received 20 January 1989

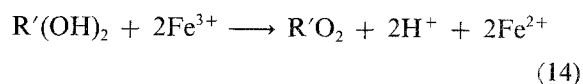
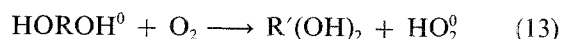
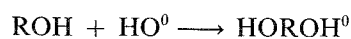
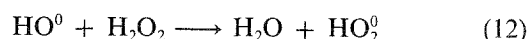
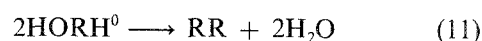
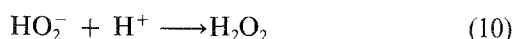
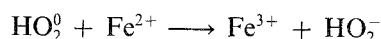
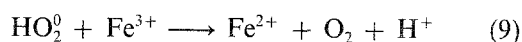
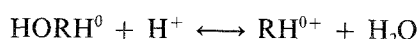
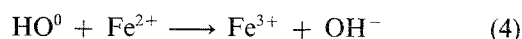
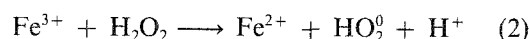
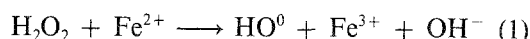
Fenton's reagent, regenerated by the electrochemical reduction $\text{Fe}^{3+} + e^- \longrightarrow \text{Fe}^{2+}$ has been used for the hydroxylation of benzene into phenol in both continuous and batch processes. In a batch process, the current yield for this reaction is relatively low because of the oxidation, in the aqueous phase, of phenol and its oxidation products by HO^0 radicals. When the phenol is continuously extracted in the form of phenate ions, the current yield is found to increase from 20 to 70% for a nine-fold rise in the rate of benzene circulation. Varying the sulphuric acid concentration in the range 0.05 to 0.8 M has little effect on current yield, while varying the Fe^{3+} concentration gives a maximum yield of about 70% for a concentration of 0.1 M. At higher Fe^{3+} concentrations the rate of production of HO^0 radicals becomes too high in comparison with the rate of benzene hydroxylation. The presence of a co-solvent like CCl_4 , although unreactive with HO^0 , reduces the yield. A numerical model taking into account the 13 reactions for which rate constants could be found or estimated, was developed for the continuous process. This model can only predict the general trends in yield and is not quantitatively predictive. Attempts at hydroxylating fluorobenzene using Fenton's reagent with electrochemical regeneration did not give appreciable yields of fluorophenols.

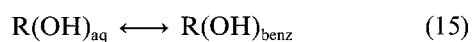
1. Introduction

Fenton's reagent (FR) is a mixture of hydrogen peroxide and ferrous ions which, in an aqueous medium, produces hydroxy radicals capable of oxidising a number of organic substrates. The oxidation of aromatic hydrocarbons by the hydroxy radical has undergone particular study; the products of this reaction are phenols. The overall hydroxylation reaction for an aromatic hydrocarbon can be represented by the following scheme:



When this reagent is prepared by mixing the two constituents, the oxidation of the substrate is difficult to control and numerous by-products are likely to be formed. Furthermore, the regeneration of the ferrous ions is not complete. As a result, it has been suggested that the ferrous ions might be reduced electrochemically [1-10]. This technique allows the rate of formation of hydroxy radicals to be controlled. Tomat and Vecchi [1] have shown that FR could be formed by reduction of ferric ions and oxygen on a mercury cathode. They studied the hydroxylation of benzene in these conditions and showed that phenol could be obtained with a current yield of 60% on the basis of 3F per mole of phenol.





In a recent publication, a numerical model was presented which described the behaviour of a batch reactor in which FR, regenerated electrochemically, was used for the hydroxylation of benzene to phenol [11]. The reaction scheme used in this model was based on the work of Walling *et al.* [12–15]. It is represented by Equations 1–11 in the set of Reactions 1–15.

The principal steps in this sequence are: first, Reaction (1) between the hydrogen peroxide and the ferrous ion which forms the hydroxy radical; then the addition (3) of the radical onto the aromatic ring to give the hydroxycyclohexadienyl radical; then the oxidation of this radical to phenol by oxygen (6), when it is present, or by the ferric ion (7). Reaction (6) is much faster than Reaction (7); it gives the hydroperoxy radical which can be either oxidised by the Fe^{3+} ion (9) or reduced by the Fe^{2+} ion (10).

On the other hand, side reactions occur which consume HO radicals either by dimerisation (5), by oxidation of the ferrous ion (4) or by reaction with hydrogen peroxide (12). Another side reaction leads to the formation of biphenyl. The numerical study [11] shows that, in the case of the hydroxylation of benzene, the loss of selectivity due to the formation of biphenyl (11) is relatively slight.

The formation of polyphenols has also been mentioned, as well as reactions which open the aromatic ring, but this aspect of oxidation reactions with FR is very complex and has been scarcely studied [9, 16–20].

On the whole, the reactions between FR and aromatic hydrocarbons are complex and highly sensitive to the experimental conditions. The present work was undertaken with the aim of studying the influence of operating parameters, such as concentrations and flow rates, on the selectivity of the hydroxylation of benzene by FR regenerated electrochemically. This test reaction was studied using first of all a batch reactor and, secondly, an apparatus operating continuously with extraction of the phenol. The experimental results are compared with the predictions of a numerical model derived from the above reaction scheme and adapted to the conditions of electrolysis with continuous extraction. An attempted application to the synthesis of hydroxyfluorobenzene is also mentioned.

2. Experimental

2.1. Batch system

The batch electrolyses are performed in a 500 ml cylindrical glass reactor (CGR), containing 400 ml of an aqueous solution of sulphuric acid and ferric sulphate, in which the benzene (25 ml) is dispersed by stirring. The aqueous solution is thus permanently saturated with benzene.

The working electrode consists of a 32 cm² mercury pool stirred on the surface by a magnetic stirrer. The anode is a platinised titanium plate (IMI Titanium, United Kingdom), rolled into a cylinder. The two

compartments are separated by a ceramic diaphragm (Schumacher, Federal Rep. Germany). The cathode potential is measured with respect to a saturated calomel electrode (SCE). A flexible Teflon catheter, 1 mm in diameter (Denucath, Plastimed, France), containing a conducting agar–agar gel, one end of which is fixed to a syringe carrying the SCE while the other is placed near the working electrode, allows electrolyses to be performed at fixed potentials.

During the electrolyses, the aqueous solution is kept saturated with oxygen, while hydrogen peroxide may or may not be added. When it is used, the injection of hydrogen peroxide begins 10 min after the beginning of the electrolysis, with a flow rate whose value depends on the initial current. This flow rate is calculated by considering that, at the value of the working potential chosen, the whole of the current is used to regenerate the ferrous ion.

At the end of the electrolysis, the aqueous solution is treated with ether. After separation, the ether is dried then evaporated; the residue is analysed by gas-phase chromatography (GPC) using a column packed with an SE 30 stationary phase. The products are identified by their retention time. In quantitative analysis, toluene is used as internal standard and the detector is a thermal-conductivity detector (TCD).

2.2. Continuous system

In order to avoid the accumulation of phenol in the benzene–water suspension, an electrolysis set-up with continuous extraction of the phenol was used. This apparatus, shown in Fig. 1, consists of three liquid loops in contact. In the first circuit, the aqueous phase saturated with oxygen circulates between the electrochemical reactor 1, where the ferrous ions are regenerated, and the chemical reactor 2 into which the hydrogen peroxide is injected at a rate fixed according to the current used in converting Fe^{3+} to Fe^{2+} . In the second loop, the benzene is first dispersed in the stirred chemical reactor 2 to saturate the aqueous phase, then after passing through the plug reactor 3, is separated by gravity in the settler 4 and finally put into contact with the aqueous NaOH solution which circulates in the third loop (5 and 6) gradually getting richer in phenate ion.

An identical apparatus was used for a series of experiments on the synthesis of fluorophenols. However a device for separating fluorobenzene by distillation has also been used. The set-up is the same as that described in Fig. 1, except for part 5. At the outlet of the settler 4, part of the fluorobenzene is sent off for distillation 5, the rest being recycled into reactor 2 via the by-pass 7. At the end of the reaction, the whole of the fluorobenzene is distilled. The residue from the distillation is analysed by liquid-phase chromatography (HPLC) by the method described below.

The electrolysis cell 1 is of the filter-press type (Micro Flow Cell, Electro Cell AB, Sweden). The area of the working electrode is 13 cm². The anode is of platinised titanium (DSA) and the cathode chosen is

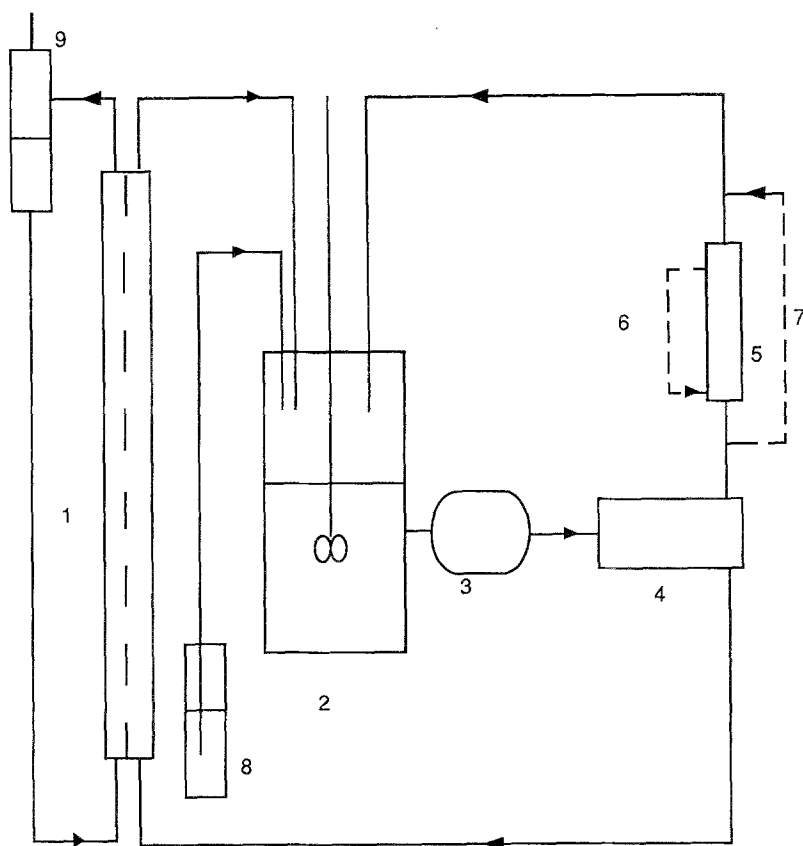


Fig. 1. Experimental apparatus for the continuous oxidation of aromatic compounds by FR; 1, divided electrolytic cell; 2, continuously stirred chemical reactor; 3, plug flow reactor; 4, horizontal decanter; 5, separator (continuous extraction by sodium hydroxide or distillation column); 6, recycle of sodium hydroxide; 7, by-pass; 8, H_2O_2 tank; 9, oxygen separator. Oxidation of benzene: Aqueous phase: 0.21 0.1 M to 1 M H_2SO_4 ; 0.005 to 0.2 M Fe^{3+} ; saturated with O_2 (~ 1 mM); flow rate: 2–15 l h^{-1} . Organic phase: 11 benzene; 10–30 l h^{-1} . Extraction: 0.151 1 M NaOH; 10 l h^{-1} . Oxidation of fluorobenzene: Aqueous phase: 0.21 0.6 M H_2SO_4 or 0.05 to 0.5 M HClO_4 ; 0.007 to 0.05 M Fe^{3+} ; saturated with O_2 (~ 1 mM); flow rate: 2 l h^{-1} . Organic phase: 11 fluorobenzene; total flow-rate: 21 l h^{-1} ; submitted to distillation: 0.91 l h^{-1} .

of vitreous carbon (VC). A Nafion 423 ion-exchange membrane separates the two compartments.

Current-potential curves were plotted with this cell using a flexible catheter similar to the one previously described. The catheter passes through the tube through which the electrolyte enters the cathode compartment and its end is placed in contact with the working electrode.

The continuously stirred reactor 2 consists of a 500 ml glass cylinder (SVL, Sovirel, France). The two phases are vigorously stirred so as to obtain a suspension in which the benzene droplets have a diameter of the order of 0.1 to 0.5 mm. This suspension, on the one hand, keeps the electrolyte solution saturated with benzene and, on the other, performs the continuous extraction of the phenol from the aqueous phase. The equilibrium constant for the distribution of phenol between the benzene and the aqueous solution used (0.6 M H_2SO_4 ; 0.05 M $\text{Fe}_2(\text{SO}_4)_3$) was measured and found to be 3.5 at 20°C.

All the reagents are initially charged into the stirred reactor. A plug flow reactor 3, consisting of a glass tube 4 m long, is placed at the outlet. This reactor, whose length was estimated from the kinetic data collected in reference [11], allows the reagents H_2O_2 and Fe^{2+} to be almost completely used up.

At the end of the electrolysis, the NaOH having circulated in the loop 5–6 (Fig. 1) is neutralised. The acidified solution is then treated with ether as described above. The extracted products were analysed by liquid-phase chromatography (HPLC) with C18 inverse phase. The detection was by UV absorption at 270 nm. The carrier is a 25% by volume aqueous methanol

solution buffered at pH 2 by a mixture of HCl and KCl.

3. Results and discussion

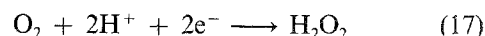
3.1. Oxidation of benzene

3.1.1. Batch operation: electrolyses with a mercury pool. The current-potential curves for the reduction of the ferric ion and of oxygen on a mercury pool in a 0.6 M H_2SO_4 solution are shown in Fig. 2. The curve for the reduction of Fe^{3+} on the stirred mercury pool shown two parts: the first, situated between -0.4 and -0.9 V versus SCE, is reproducible; it corresponds to the reduction of Fe^{3+} to Fe^{2+} . The peak situated between 0.0 and -0.4 V has not been closely studied, but it is apparently related to adsorption phenomena.

With a stirred mercury pool of this sort, a single wave, spread over 600 mV, is observed for the reduction of oxygen. This wave ends on a plateau of diffusive origin which is associated with the overall reaction:



However, the electrolysis at $E = -0.30$ V versus SCE of a 0.6 M sulphuric acid solution saturated with oxygen gives hydrogen peroxide, according to the reaction:



The hydrogen peroxide solution is titrated with cerium IV; the current yield is 55%.

The preparative electrolyses in the presence of

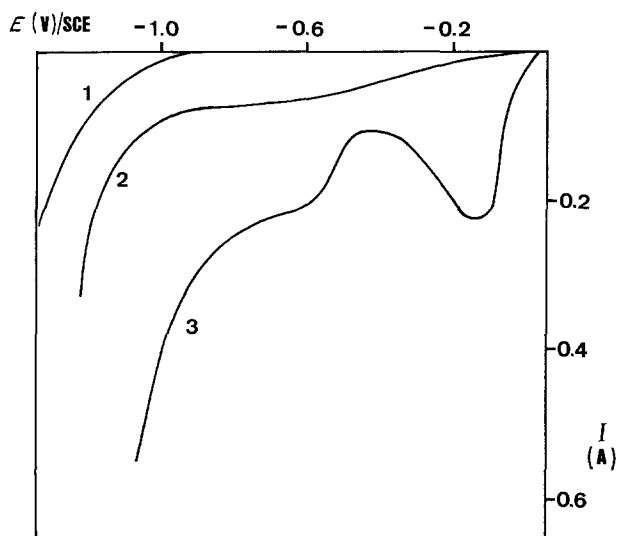


Fig. 2. Current-potential curves on mercury pool (32 cm²) in 0.6 M H₂SO₄ at 500 m V mn⁻¹; t: 25°C; (1) residual; (2) 1 mM O₂; (3) 0.01 M Fe₂(SO₄)₃.

benzene were performed at controlled potential. The current yield used below is defined in two ways, depending on the operating conditions used:

– when the hydrogen peroxide is derived solely from the 2e⁻ reduction of oxygen, 3 F are required to produce one mole of H₂O₂ and one mole of Fe²⁺:

$$\eta_f = 3 F n_p / Q \quad (\text{I})$$

where n_p represents the quantity of phenol formed and Q the total charge having passed during the electrolysis;

– when hydrogen peroxide is added to the reaction medium, the yield is defined with respect to the quantity of charge required to regenerate the ferrous ion:

$$\eta_f = F n_p / Q \quad (\text{II})$$

The results of the electrolyses are summarised in Table 1.

No dihydroxylated products were found in the ether extraction residues when analysed by GPC with a TCD. Also, the quantities of biphenyl formed were always small and where there is no addition of hydrogen peroxide, they decreased as the ferric ion

concentration increased. This indicates that the cyclohexadienyl radical is oxidised more quickly by Reactions 6 and 7 than it can disappear by Reaction 11.

The maximum value for the current yield in phenol is never greater than 28% when the hydrogen peroxide is formed by reduction of oxygen at the cathode and can be as high as 38% when hydrogen peroxide is added to the reactor. Furthermore, an increase in phenol current yield is observed when the initial iron concentration decreases.

In fact, when the hydrogen peroxide is formed by the 2e⁻ reduction of oxygen (17), its rate of formation is limited by the low solubility of oxygen in the aqueous phase (approximately 0.001 mol l⁻¹). For Experiments 1 to 3 (Table 1), performed at oxygen saturation and without addition of hydrogen peroxide, the phenol yield increases when the initial iron concentration decreases from 0.01 M to 0.0005 M. Tomat and Vecchi [1] performed a systematic study of the influence of the iron concentration and found a maximum yield for an Fe³⁺ concentration of 0.005 M. These authors suggested that this maximum was due to the rate of ferrous ion formation being equal to the rate of formation of hydrogen peroxide.

The most favourable operating conditions can be obtained when the hydrogen peroxide enters the reactor at a molar flow rate equal to the rate of regeneration of the ferrous ion. However, it is difficult to judge the right rate of addition because of the possibility, in the presence of dissolved oxygen, of hydrogen peroxide being formed at the cathode and because of the possibility of ferrous ions being regenerated chemically. In our experiments, the rate of addition of hydrogen peroxide was determined from the initial value of the reduction current. It is under these conditions that the highest current yield was observed (Experiment 4 in Table 1); the improvement, however, is modest since the best yield observed is 38%. Moreover, the yield falls off at a higher Fe III concentration (Experiment 5), while in the absence of oxygen it drops sharply (Experiments 6 and 7).

This low current yield most likely results from the accumulation of phenol in the aqueous phase which leads to its oxidation by the HO radicals. This causes a decrease in selectivity of the reaction as the phenol is itself oxidised by FR [9, 16–20]. The rate of this side

Table 1. Results of electrolyses on a mercury pool (32 cm²) in batch operation at 25°C. Potentiostatic conditions: -0.3 V/SCE; (*) -0.6 V. Aqueous phase: 400 cm³ of 0.6 M H₂SO₄. Organic phase: 25 cm³ benzene. Analysis by GPC

RUN N ^o	O ₂	H ₂ O ₂ (M)	Fe ³⁺ (M)	Q (C)	η PhOH 3 F/mol	η PhOH 1 F/mol	η Ph-Ph 6 F/mol	η Ph-Ph 2 F/mol
1	yes	-	0.0005	453	27.8	-	6	-
2	yes	-	0.002	2100	21	-	3	-
3	yes	-	0.01	1540	6.8	-	<1	-
4	yes	yes	0.0003	130	-	38	-	3
5 (*)	yes	yes	0.01	1737	-	15	-	<1
6	no	yes	0.01	684	-	8	-	2
7	no	yes	0.01	540	-	7	-	-

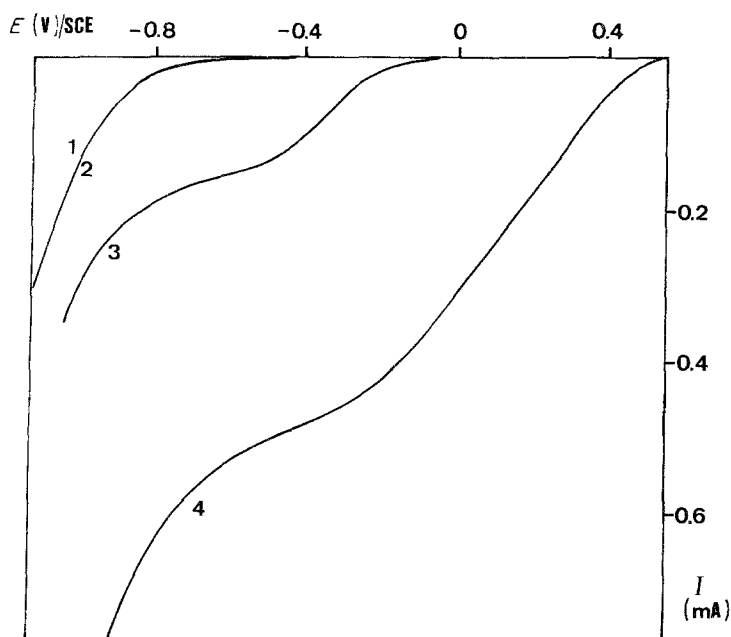


Fig. 3. Current-potential curves on a rotating vitreous carbon disk electrode ($d: 4 \text{ mm}$) at 500 m V min^{-1} ; in $0.6 \text{ M H}_2\text{SO}_4$; $\omega: 2000 \text{ t min}^{-1}$; $t: 25^\circ \text{ C}$; (1) residual; (2) 0.012 to $0.14 \text{ M H}_2\text{O}_2$; (3) 1 mM O_2 ; (4) $0.01 \text{ M Fe}_2(\text{SO}_4)_3$.

reaction increases during the electrolysis as the phenol accumulates in the aqueous phase. The dihydroxybenzenes thus formed are themselves oxidised by the ferric ion (section 3.2.). Even though the analysis by GPC did not show up any dihydroxylated products after these electrolyses, it is likely that these products are in fact formed. During the electrolyses, the electrolyte solution takes on a brown colour which darkens as the amount of charge having passed increases. An identical colour is obtained when a solution of ferric ions is mixed with an acidified solution of polyphenols.

This preliminary study showed that the rate of formation of FR is extremely slow when the hydrogen peroxide is formed by cathodic reduction of the dissolved oxygen because of the low solubility of this gas in aqueous solutions. Also, the accumulation of the phenol in the aqueous phase is probably responsible for the side reactions which reduce the selectivity of the reaction. Thus the phenol must be extracted from the medium progressively as it is formed.

3.1.2. Continuous operations: electrolyses with the filter-press cell. The curves for the reduction of Fe^{3+} , oxygen and hydrogen peroxide are shown in Fig. 3. These curves were plotted using a vitreous carbon rotating disk. The oxygen reduction begins at about -0.2 V and takes place in a single wave. For the sake of comparison, the same curves were plotted under identical conditions using a vitreous carbon cathode in the filter-press cell; a single wave was also observed in this case. The reduction of the ferric ion begins at about 0.5 V and shows a diffusion plateau between -0.4 and -0.8 V (Fig. 3, curve 4). However, curve 2 of Fig. 3 shows that the hydrogen peroxide is not reduced on vitreous carbon. This implies that the reduction wave for oxygen on vitreous carbon corresponds to Reaction (17) involving two electrons.

The electrolysis experiments were performed with

the set-up shown in Fig. 1 with hydrogen peroxide being added at a constant rate to the continuously stirred reactor. The concentrated solution flowing drop by drop into the reactor is immediately dispersed throughout the suspension into which the regenerated iron solution is returned after passing through the electrolysis cell. The aqueous solution is kept saturated with oxygen at ambient temperature ($20 \pm 1^\circ \text{ C}$). The current yield used in the following discussion is the one given by Equation (II).

The material yield is defined with respect to the hydrogen peroxide added to the reactor:

$$\eta_m = n_p/n_r \quad (\text{III})$$

where n_r is the quantity of hydrogen peroxide consumed.

(a) *Influence of the ferric ion concentration.* Figure 4 shows the variations in current and material yield for phenol, as a function of ferric ion concentrations in the range 0.005 to 0.2 M . It can be seen that the current yield increases significantly between 0.005 and 0.1 M , then passes through a maximum of about 70% at 0.1 M then decreases from 0.1 and 0.2 M . Now for each experiment shown on Fig. 4, the rate of formation of Fe^{2+} ions and the rate of addition of hydrogen peroxide are of the same order of magnitude. Moreover all the electrolyses were performed with solutions saturated with oxygen at the inlet to the electrochemical reactor. Thus at the working potential used in these electrolyses (-0.6 V versus SCE), the oxygen and the iron are reduced simultaneously (Fig. 3) and the potential is situated on the diffusion plateaux of the current-potential curves. At low iron concentrations, the reduction current for the oxygen is not a negligible fraction of the overall current. For example, for a ferric ion concentration of 0.01 M , the oxygen reduction current at 20° C represents 28% of the total current (Fig. 3). At the chosen working potential, as the kinetic regime of the two reactions is diffusive,

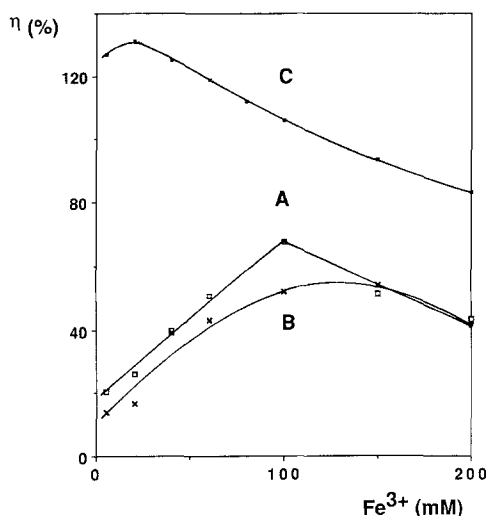


Fig. 4. Phenol yield- Fe^{3+} concentration plots. Electrochemical regeneration of Fe^{2+} in a filter-press cell; VC cathode 13 cm^2 . Potentiostatic conditions: $E = -0.6 \text{ V/SCE}$; $t: 20^\circ \text{C}$; Anode DSA; Catholyte: 0.21 of 0.6 M H_2SO_4 saturated with O_2 ($\sim 1 \text{ mM}$); flow rate: 21 h^{-1} . Organic phase: 1:1 benzene; flow rate: 191 h^{-1} . (A) Current yield (on 1 F basis); (B) Chemical yield; (C) theoretical current yield from numerical model.

when the iron concentration increases, the relative share of the oxygen reduction current decreases and the current yield increases.

When the ferric ion concentration exceeds 0.1 M, the current yield in phenol decreases. In this region, it seems that the rate of formation of hydroxy radicals becomes sufficiently high for these radicals to accumulate in the aqueous phase because of the limited solubility of benzene in this phase. These radicals are then destroyed by Reactions (4), (5) and (12), or else they react with the phenol according to Reaction (13). This reaction has been taken into account in the numerical

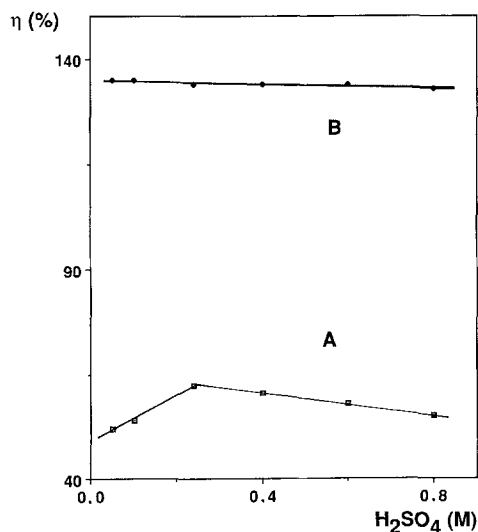


Fig. 5. Phenol yield- H_2SO_4 concentration plots. Electrochemical regeneration of Fe^{2+} in a filter-press cell; VC cathode 13 cm^2 . Potentiostatic conditions: $E = -0.6 \text{ V/SCE}$; $t: 20^\circ \text{C}$; Anode DSA; Catholyte: 0.21 of aqueous 0.1 M Fe^{3+} , saturated with O_2 ($\sim 1 \text{ mM}$); flow rate: 21 h^{-1} . Organic phase: 1:1 benzene; flow rate: 11.41 h^{-1} . (A) Current yield; (B) theoretical current yield from numerical model.

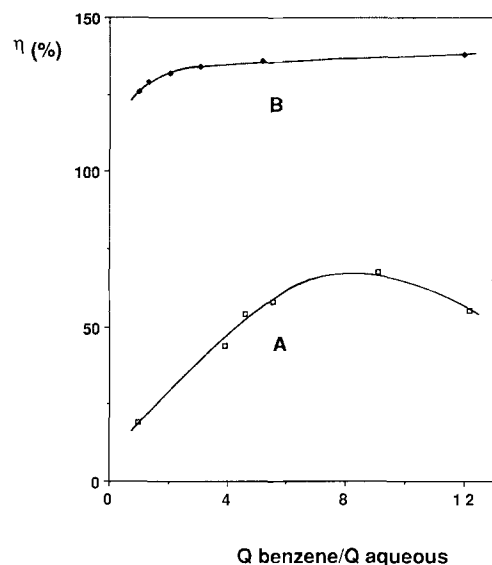


Fig. 6. Current yield in Phenol-organic/aqueous flow rates ratio plots. Electrochemical regeneration of Fe^{2+} in a filter-press cell; VC cathode 13 cm^2 . Potentiostatic conditions: $E = -0.6 \text{ V/SCE}$; $t: 20^\circ \text{C}$; Anode DSA. Catholyte: 0.21 of 0.6 M H_2SO_4 and 0.1 M Fe^{3+} saturated with O_2 ($\sim 1 \text{ mM}$); flow rate: 41 h^{-1} . Organic phase: 1:1 benzene; (A) Current yield; (B) theoretical current yield from numerical model.

model even though the rate constant available [21] was not measured in an acid solution.

(b) *Influence of the acidity of the medium.* Electrolyses were performed for sulphuric acid concentrations ranging from 0.05 M to 0.8 M. The variations in current yield are shown in Fig. 5. The curve passes through a slight maximum at H_2SO_4 concentration of the order of 0.3 M.

When the acid concentration is reduced, Reaction (1) is less favored while step (2) is on the contrary facilitated. This results in a disappearance of the hydrogen peroxide and a fall in yield. On the other hand, when the acid concentration increases, the equilibrium (8) is shifted, thus leading to a more rapid destruction of the cyclohexadienyl radical cation with a return to benzene. However, since the constant k_2 is lower than k_1 , with k_8 much lower than k_6 [11], the result is that the acidity has only a weak influence on the yield, at least in the range studied.

(c) *Influence of the rate of circulation of the benzene.* The effect of varying the flow rate of benzene in the stirred reactor was studied for an iron concentration of 0.1 M, the value which gave the highest current yield in the previous experiments. Preliminary tests showed that the stripping of the benzene stream, with a 1 M sodium hydroxide solution, was effective throughout the whole electrolysis time.

Figure 6 shows that the phenol current yield goes from 20% to 70% when the benzene flow rate is multiplied by 9, with all other parameters being held constant. If one assumes that the phase equilibrium (15) is respected at all time in the benzene-water suspension, it can be deduced that this improvement in yield results from the increase in the rate of phenol extraction due to the higher benzene flow rate. However, when the flow-rate ratio is increased beyond 10,

Table 2. Results of continuous electrolyses with CCl_4 as a co-solvent. Electrochemical regeneration of Fe^{2+} in a filter-press cell: VC cathode 13 cm^2 . Potentiostatic conditions: $E = -0.6\text{ V/SCE}$; $t: 25^\circ\text{ C}$; Anode DSA. Aqueous phase: 0.21 of $0.6\text{ M H}_2\text{SO}_4$ with 0.1 M Fe^{3+} saturated with O_2 ($\sim 1\text{ mM}$); flow rate: 21 h^{-1} . Organic phase: 11 benzene; flow rate: 11.71 h^{-1} . Extraction of phenol with 1 M NaOH . Analysis by GPC

$\text{H}_2\text{O}_2 \times 10^6$ (mol s^{-1})	Q (C)	$V_{\text{C}_6\text{H}_6}$ (cm^3)	V_{CCl_4} (cm^3)	η (%) 1 F mol^{-1} PhOH
1.483	1645	1000	–	44
1.246	966	800	100	20
1.389	792	800	200	< 1

for an aqueous-phase flow rate of 41/hour, there is a decrease in phenol current yield. It should be noted that at this value of the benzene flow rate, the installation becomes inefficient due to flooding of the settler. This causes the sodium hydroxide solution to be carried over into the stirred reactor.

(d) *Effect of a co-solvent.* With the aim of improving the equilibrium constant for the phenol between the organic phase and the aqueous phase, experiments were performed with tetrachloromethane added to the benzene. This solvent was chosen because of its low reactivity with respect to hydroxy radicals [21]. The results obtained are given in Table 2. It is obvious that this co-solvent gives no improvement. On the contrary, lower performances are obtained in these conditions. In fact the presence of the CCl_4 increases the solubility of phenol in the organic phase but reduces the solubility of benzene in water, thus leading to a loss HO radicals (Reactions 4 and 5).

(e) *Comparison with the predictions of the numerical model.* A numerical model taking into account the Reactions (1–13) was developed as an aid in interpreting the operation of the set-up with continuous extraction of phenol [11]. This model has been applied to the case where a stirred chemical reactor is coupled with the electrochemical reactor so as to optimize the conditions for the synthesis of phenol (see Appendix). The effect of varying the initial iron concentration, the effect of the acidity and the effect of the ratio of the flow rates of the organic and aqueous phases are shown in Figs 4, 5 and 6. The results from the model show a variation analogous to that observed experimentally. However the figures show a difference close to 100% between the predicted and the experimentally observed current yields. This shows that the model used, though very complex, does not take into account all of the reactions. And the rate constants for some reactions (in particular, the oxidation of phenol) are not exactly known.

Furthermore, no data concerning the kinetics of the reactions between FR and the products of the oxidation of phenol (such as quinones) have been published [21]; the reaction mechanism seems however to be extremely complex [18–20]. It is likely that the observed loss of yield is due to FR being consumed in

these reactions. The action of FR on phenol and on quinone was examined.

3.2. Oxidation of phenol and quinone

The yields obtained in the preceding experiments, which are quite low in comparison with the theoretical predictions, can be explained on the one hand by the reaction in the aqueous phase of FR on the phenol and its oxidation products and on the other by a loss of HO radicals. This reactivity of the phenol results from its partial solubility in the aqueous phase. Also, the phase equilibrium for the phenol in the two phases was apparently not reached instantaneously, so its concentration in the aqueous phase should be higher than its equilibrium value.

The reaction of FR with phenol was studied by various authors [3, 9, 16–20]. Phenol can be completely destroyed by FR under certain conditions [18, 20]. In particular, by varying the initial concentration ratios $[\text{H}_2\text{O}_2]_0/[\text{Fe}^{2+}]_0$ and $[\text{H}_2\text{O}_2]_0/[\text{PhOH}]_0$, phenol can be oxidized preferentially either to pyrocatechol or to hydroquinone [18].

During this work on the oxidation of phenol, FR was formed electrochemically in a filter-press cell, with 350 ml of a $0.6\text{ M H}_2\text{SO}_4$ solution saturated with oxygen, containing 0.01 M Fe^{3+} and 0.152 M PhOH . In an electrolysis at -0.6 V versus SCE, the reduction current for the Fe^{3+} requires an addition of H_2O_2 at the rate of $3.11 \times 10^{-7}\text{ mol s}^{-1}$.

The progress of the reaction is followed by HPLC. Analysis of samples taken at various times have shown that for an electrolysis period of less than three hours, only quinone can be detected. This can be easily explained if the rate of hydroxylation of phenol $k_{\text{ROH}}[\text{ROH}][\text{HO}]$ is greater than the rate of oxidation of the quinone $k_{\text{Q}}[\text{Q}][\text{HO}]$. It may thus be assumed that Reactions (13) and (14) take place once the benzene has been hydroxylated. It should further be noted that the solution takes on a brown colouring apparently due to complexes between the Fe^{3+} and the quinone. During the oxidation of benzene, therefore, part of the phenol formed is hydroxylated to polyphenols. However, during this work, these products have never been observed. The absence of polyphenols thus implies that quinones are formed by oxidation by the Fe^{3+} . This reaction is thermodynamically possible at the pH levels used. The potential for the redox pair $\text{Fe}^{2+}/\text{Fe}^{3+}$ is 0.95 V versus NHE for $[\text{Fe}^{3+}] = 0.1\text{ M}$ and $[\text{Fe}^{2+}] = 10^{-4}\text{ M}$, whereas for the pair quinone/hydroquinone the redox potential is 0.693 V when $[\text{Q}] = [\text{H}_2\text{Q}]$ in a $[\text{H}^+] = 0.8\text{ M}$ medium.

The apparatus used did not allow a complete reaction balance to be performed because of the difficulty in recovering all of the quinone which precipitates ($C_{\text{sat}} \approx 0.01\text{ M}$). Also, when the electrolysis is continued beyond 200 min, unidentified products having a small number of carbon atoms are found to be present.

Still with the aim of interpreting the low yields obtained in the hydroxylation of benzene, the action of FR on quinone was examined and the stoichiometry

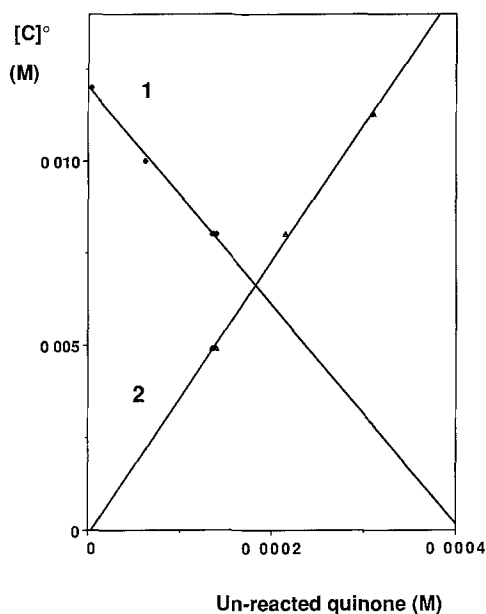
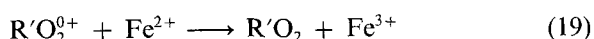
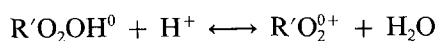
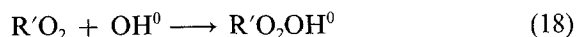


Fig. 7. Un-reacted quinone concentrations as a function of initial concentration of H_2O_2 and Fe^{2+} ; 1 $[\text{Fe}^{2+}]$: 4.9 mM; $[\text{Quinone}]$: 2.6 mM; 2 $[\text{H}_2\text{O}_2]$: 8 mM; $[\text{Quinone}]$: 12.15 mM.

of the reaction was measured. Preliminary tests showed that hydrogen peroxide alone only reacts very slowly with quinone. For example, when a quinone solution (0.012 M) is mixed with a hydrogen peroxide solution (0.026 M) at 6°C and at $\text{pH} = 2$, HPLC analysis reveals no modification in quinone concentration with time. Figure 7 shows the variation in the quantity of residual quinone after addition of a $\text{H}_2\text{O}_2 + \text{Fe}^{2+}$ mixture, as a function of the initial concentrations of iron and hydrogen peroxide. The reaction is rapid (a few seconds) and the quantity of quinone remaining does not vary in time. The intercept of curve 1 on the axis in Fig. 7 gives the quantity of hydrogen peroxide necessary to consume the whole of the quinone. To oxidise one molecule of quinone, 4.6 molecules of H_2O_2 are required. This suggests that the aromatic cycle is broken. Aliphatic compounds are formed; in particular, various acids which we have not been able to identify. The compounds formed can themselves be oxidized. It has been shown [20] that muconic acid is formed by the breaking of the quinone ring. Acids having a low number of carbon atoms have been previously detected [18]. As a result, one quinone molecule consumes a large number of HO radicals; this explains the low current yields obtained during the electrolyses.

Curve 2 of Fig. 7 shows a rise in the amount of residual quinone with increasing initial Fe^{2+} concentrations. There are two reasons for this phenomenon:

– there can be consumption of Fe^{2+} with simultaneous regeneration of a quinone molecule $\text{R}'\text{O}_2$ according to a reaction similar to (8):

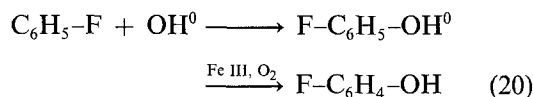


The rate of this reaction increases with the Fe^{2+} concentration.

– the mixture of hydrogen peroxide and Fe^{2+} at high concentrations leads to an accumulation of HO radicals. This causes the destruction of part of these radicals by Reactions (4), (5) and (12).

3.3. Oxidation of fluorobenzene

An attempt has been made to apply to fluorobenzene the results obtained with benzene. The development of an experimental device and the optimization of parameters such as the Fe^{3+} concentration, made it possible to envisage an application to the synthesis of fluorophenol:



The synthesis of fluorophenols by FR has been considered by previous authors [7, 8]. They performed the reaction in a two-phase medium: fluorophenol-aqueous phase, containing HClO_4 and Fe^{3+} or Cu^{2+} and carried out the continuous separation of the products by distillation of the organic phase. The current yields quoted [7] are as high as 430% (85% ortho, 15% para).

The results of preparative electrolyses with extraction by sodium hydroxide are listed in Table 3. The formation of fluorophenols was not observed. However, the analyses (GPC and HPLC) show the formation of phenol with a current yield between 10 and 75%. It should be noted that this phenol comes from the action of FR, and not sodium hydroxide, on the fluorobenzene. Reactivity tests performed with fluorobenzene and sodium hydroxide under the conditions used in these experiments were negative. On the other hand, the HPLC analysis of the sodium hydroxide stripping solution shows the presence of an intense peak which we have not been able to identify with certainty. However, since on the one hand this signal is not observed with the TCD (as for the quinones) and on the other, the HPLC retention time is very close to that of parabenzoquinone, it could well be due to fluoroquinones coming from the successive steps in the oxidation of fluorophenol by the HO radical. The possibility of there being polyphenols present cannot be considered, because of their reductive nature with respect to the ferric ion in acid media.

To stop quinone-like compounds from being recycled into the reactor, a device for continuous separation by distillation of the fluorophenol was worked out (Fig. 1). The results of the preparative electrolysis trials are given in Table 4. HPLC analysis of the distillation residue indicates the formation of traces of fluorophenols (current yields $< 3\%$). Phenol is still obtained with a yield between 9 and 40%. In the chromatogram, there is a peak identical to the one previously obtained, but its intensity is even greater. Tests performed by varying the Fe^{3+} concentration, the nature of the oxidant (Fe^{3+} , Cu^{2+} and O_2), the

Table 3. Results of attempts at preparative electrolysis for fluorophenol. *t*: 25°C Aqueous phase: 0.2l; flow rate: 21h⁻¹. Organic phase: 1.1l fluorobenzene; flow rate: 201h⁻¹. Extraction of fluorophenols with 5 M NaOH. Analysis by HPLC. (*) formation of an unidentified product. (**) GPC analysis

<i>E</i> (V)/SCE	<i>C</i> _{FeIII} (M)	Acid	Gas	<i>H</i> ₂ <i>O</i> ₂ addition × 10 ⁷ (mols ⁻¹)	<i>Q</i> (C)	Oxidant	Remarks
-0.6	0.098	1 M H ₂ SO ₄	O ₂	3.52	1 120	Fe ³⁺	No fluorophenols 10% yield in phenol (*)
-0.6	0.150	1 M H ₂ SO ₄	O ₂	14.95	1 165	Fe ³⁺	No fluorophenols 25% yield in phenol (*)
-0.6	0.010	1 M H ₂ SO ₄	O ₂	1.24	231	Fe ³⁺	No fluorophenols 74% yield in phenol (*)
-0.2	0.010	1 M H ₂ SO ₄	N ₂	1.404	235	0.01 M Cu ²⁺	No fluorophenols (**)
-0.05	0.100	0.1 M HClO ₄	N ₂	18.58	840	0.01 M Cu ²⁺	No fluorophenols (**)

concentration and nature of the acid (H₂SO₄, HClO₄) did not allow appreciable yields of fluorophenol to be obtained.

In short, the results of numerous experiments performed under varied operating conditions and using two different separation techniques have not shown that significant quantities of fluorophenols could be formed; this is in contradiction with results published previously [7, 8].

4. Conclusion

It appears from this work that FR is an extremely reactive system and its reaction mechanism is very complex. The HO radicals can react with a large number of molecules and one, two or more hydroxylation steps can occur.

This work shows that it is essential to remove the product from the reaction medium in order to protect

Table 4. Results of attempts at preparative electrolysis for fluorophenol. *t*: 25°C Aqueous phase: 0.2l; flow rate: 21h⁻¹. Organic phase: 1.1l fluorobenzene; flow rate: 201h⁻¹. Continuous separation by distillation; flow rate: 0.91h⁻¹ of fluorobenzene. HPLC analysis. (*) formation of an unidentified product

<i>E</i> (V)/SCE	<i>C</i> _{FeIII} (M)	Acid	Gas	<i>H</i> ₂ <i>O</i> ₂ addition × 10 ⁷ (mols ⁻¹)	<i>Q</i> (C)	Oxidant	Remarks
-0.6	0.050	0.6 M H ₂ SO ₄	O ₂	8.7	1 100	Fe ³⁺	2% yield in fluo- rophenols 11% yield in phenol (*)
-0.6	0.050	0.6 M H ₂ SO ₄	O ₂	11.11	1 425	Fe ³⁺	2.5% yield in fluorophenols 9.7% yield in phenol (*)
-0.6	0.007	0.6 M H ₂ SO ₄	O ₂	3.19	650	Fe ³⁺	fluorophenol traces 9.3% yield in phenol (*)
0.1	0.007	0.6 M H ₂ SO ₄	N ₂	1.04	97	Cu ²⁺ 0.007 M	fluorophenol traces 39% yield in phenol (*)
0.1	0.007	0.5 M HClO ₄	N ₂	0.455	55	0.007 M Cu ²⁺	fluorophenol traces 37% yield in phenol
0.1	0.007	0.052 HClO ₄	N ₂	0.911	99	0.007 M Cu ²⁺	2% yield in fluorophenols 19.8% yield in phenol (*)
I constant 0.032 A	0.007	0.052 HClO ₄	N ₂	3.31	293	0.007 M Cu ²⁺	fluorophenols and phenol traces

it from further attack. Saturating the aqueous solution with the benzene substrate (0.022 M) by using vigorous stirring to form a suspension, makes it possible to increase the overall rate of oxidation of benzene in preference to other substances.

A distinct improvement in yield was obtained by going over from a batch system to a continuous system in which the phenol is rapidly transferred from the aqueous phase to the organic phase, which is then stripped by a sodium hydroxide solution. It has been shown experimentally that there is an optimum value for the ratio of the flow rates of the organic and aqueous phases.

Care should be taken to adjust parameters such as ferric ion concentration and electrode current, to avoid accumulation of HO radicals and their destruction in side reactions.

FR is an oxidizing system whose regeneration is theoretically self-sustained by rapidly extracting the product of the first hydroxylation. When the regeneration takes place at a cathode, current yields greater than 100% should be possible. In the case of the hydroxylation of benzene, the best current yields obtained were no higher than 70%. This can be explained by the presence of numerous side reactions and chain reactions that cannot be totally eliminated. These experiments confirm that the reaction mechanism used in the numerical model previously proposed [11] ought to be completed by taking into account the numerous chain reactions occurring after the formation of the phenol.

The results for the oxidation of the fluorobenzene show, on the one hand that there is formation of polyhydroxylated products and on the other, that there is an apparent substitution of the HO radical for the fluorine. It seems that none of the factors examined in this study is capable of blocking the oxidation reaction at the fluorophenol stage.

APPENDIX

Mathematics of the Numerical Model

In comparison with the reaction scheme which we previously used [11], the following changes in reaction rate formulas have been made:

$$R_8 = k_8[\text{Fe}^{2+}][\text{HORH}^0][\text{H}^+] \quad (\text{A.1})$$

$$R_{12} = k_{12}[\text{HO}^0][\text{H}_2\text{O}_2] \quad (\text{A.2})$$

$$R_{13} = k_{13}[\text{HO}^0][\text{ROH}] \quad (\text{A.3})$$

with the reaction rate constants given in Table A.1.

The vector \mathbf{r} representing the rate of formation of the different species is related to the reaction rate vector \mathbf{R} via the stoichiometric matrix $\{\mathbf{S}\}$:

$$\mathbf{r} = \{\mathbf{S}\}\mathbf{R} \quad (\text{A.4})$$

In the case of the continuous system the concentrations are calculated at three points in the circuit of the aqueous solution: (a) between the electrochemical reactor and the stirred reactor, (b) between the stirred

Table A.1. Values of the rate constants used

Reaction	Rate constant	Reference
1	$0.051 \text{ m}^3 \text{ mol}^{-1} \text{ s}^{-1}$	[12]
2	$7 \times 10^{-6} \text{ s}^{-1}$	[14]
3	$3.3 \times 10^6 \text{ m}^3 \text{ mol}^{-1} \text{ s}^{-1}$	[21]
4	$3 \times 10^5 \text{ m}^3 \text{ mol}^{-1} \text{ s}^{-1}$	[21]
5	$5.5 \times 10^6 \text{ m}^3 \text{ mol}^{-1} \text{ s}^{-1}$	[12]
6	$5 \times 10^5 \text{ m}^3 \text{ mol}^{-1} \text{ s}^{-1}$	[22]
7	$47 \text{ m}^3 \text{ mol}^{-1} \text{ s}^{-1}$	-
8	$0.55 \text{ m}^6 \text{ mol}^{-2} \text{ s}^{-1}$	-
9 and 10	$k_9 = 0.1k_{10}$	[14, 23]
11	$9 \times 10^5 \text{ m}^3 \text{ mol}^{-1} \text{ s}^{-1}$	[11]
12	$3.3 \times 10^4 \text{ m}^3 \text{ mol}^{-1} \text{ s}^{-1}$	[23]
13	$1.4 \times 10^7 \text{ m}^3 \text{ mol}^{-1} \text{ s}^{-1}$	[21]

reactor and the plug flow reactor and (c) between the plug flow reactor and the electrochemical reactor.

A mass balance on the stirred reactor gives the following relationship:

$$qc_{i|b} = qc_{i|a} + V_2 r_i + f_i \quad (\text{A.5})$$

where q is the flow rate of the aqueous phase, V_2 is the volume of aqueous phase in the reactor, f_i is the rate of addition of species i to the reactor (zero for all species except H_2O_2) and c_i is the concentration of species i . This set of non-linear simultaneous equations is solved by the Newton-Raphson method, for a given set of values for $c_{i|a}$.

The concentrations at the outlet of the plug flow reactor depend on the time taken to pass through it; this residence time τ is given by:

$$\tau = V_3/(q + q_{\text{org}}) \quad (\text{A.6})$$

where V_3 is the volume of the plug flow reactor and q_{org} is the flow rate of the organic phase. The concentrations at the outlet of this reactor are given by:

$$c_{i|c} = c_{i|b} + \int_0^\tau r_i dt \quad (\text{A.7})$$

The integration is performed by the Runge-Kutta method.

In the electrochemical reactor, only O_2 and Fe^{3+} are consumed, while only Fe^{2+} is produced. For the species consumed:

$$c_{i|a} = c_{i|c} \exp\left(-\frac{k_i A}{q}\right) \quad (\text{A.8})$$

where A is the electrode surface area and k_i is the mass-transfer coefficient for that species. For Fe^{2+} , the concentration change is calculated from the total iron concentration:

$$[\text{Fe}^{2+}]_a + [\text{Fe}^{3+}]_a = [\text{Fe}^{2+}]_c + [\text{Fe}^{3+}]_c \quad (\text{A.9})$$

It has been assumed that 50% of oxygen is reduced to H_2O according to (16), while the rest is converted to H_2O_2 according to (17).

The electrode current is given by:

$$I = qF\{[\text{Fe}^{3+}]_c - [\text{Fe}^{3+}]_a + (2x + 4(1 - x))([\text{O}_2]_c - [\text{O}_2]_a)\} \quad (\text{A.10})$$

where x is the yield in H_2O_2 for the reduction of O_2 at the electrode.

The consecutive solution of Equations (A.5), (A.7) and (A.8) starting from an initial set of concentrations $\{c_{i|a}\}_0$, will give a new value for this set of concentrations $\{c_{i|a}\}^*$. An over-relaxation factor ω is applied to this value before performing a new iteration via Equations (A.5), (A.7) and (A.8):

$$\{c_{i|a}\}_{m+1} = \omega\{c_{i|a}\}^* + (1 - \omega)\{c_{i|a}\}_m \quad (\text{A.11})$$

where $1 < \omega < 2$. The system converges satisfactorily to the steady-state solution after about forty iterations.

At each iteration, the rate of addition of H_2O_2 is calculated from the current as was explained in Section 3.2.:

$$f_{\text{H}_2\text{O}_2} = I/F \quad (\text{A.12})$$

References

- [1] R. Tomat and A. Vecchi, *J. Appl. Electrochem.* **1** (1971) 185.
- [2] R. Tomat and A. Rigo, *J. Appl. Electrochem.* **6** (1976) 257.
- [3] *Idem.*, *ibid.* **9** (1979) 301.
- [4] *Idem.*, *ibid.* **10** (1980) 549.
- [5] *Idem.*, *ibid.* **14** (1984) 1.
- [6] T. Matsue, M. Fujihira and T. Osa, *J. Electrochem. Soc.* **128** (1981) 2565.
- [7] E. Steckhan and J. Wellmann, *Angew. Chem. Int. Ed. Engl.* **15** (1976) 294.
- [8] J. Wellmann and E. Steckhan, *Chem. Ber.* **110** (1977) 3561.
- [9] B. Fleszar and A. Sobkowiak, *Electrochim. Acta* **28** (1983) 1315.
- [10] Jiin-Jiang Jow, An-Chen Lee and Tse-Chuan Chou, *J. Appl. Electrochem.* **17** (1987) 753.
- [11] M. J. Clifton and A. Savall, *J. Appl. Electrochem.* **16** (1986) 812.
- [12] C. Walling, *Acc. Chem. Res.* **8** (1975) 125.
- [13] C. Walling and S. Kato, *J. Amer. Chem. Soc.* **93** (1971) 4275.
- [14] C. Walling and A. Goosen, *ibid.* **95** (1973) 2987.
- [15] C. Walling and R. A. Johnson, *ibid.* **97** (1975) 363.
- [16] J. H. Merz and W. A. Waters, *J. Chem. Soc.* (1949) 2427.
- [17] G. Stein and J. Weiss, *J. Chem. Soc.* (1951) 3265.
- [18] N. Al-Hayek and M. Doré, *Environmental Technology Letters* **6** (1985) 37.
- [19] M. Hocking and D. Intihar, *J. Chem. Tech. Biotech.* **35A** (1985) 365.
- [20] D. Barnes, M. O'Hara, E. Samuel and D. Waters, *Environmental Technology Letters* **2** (1981) 85.
- [21] L. M. Dorfman and G. E. Adams, 'Reactivity of the Hydroxyl Radical in Aqueous Solutions', NSRDS-NBS, June 1973.
- [22] L. M. Dorfman, I. A. Taub and R. E. Bühler, *J. Chem. Phys.* **36** (1962) 3051.
- [23] C. H. Bamford and C. F. H. Tipper, 'Comprehensive Chemical Kinetics', Vol. 7, Elsevier, Amsterdam (1972) p. 564.